

Characterization of Ehp, a Secreted Complement Inhibitory Protein from *Staphylococcus aureus**

Received for publication, May 23, 2007, and in revised form, July 16, 2007 Published, JBC Papers in Press, August 15, 2007, DOI 10.1074/jbc.M704247200

Michal Hammel^{†1,2}, Georgia Sfyroera^{§1}, Serapion Pyrpassopoulos^{§1}, Daniel Ricklin^{§1}, Kasra X. Ramyar[¶], Mihai Pop^{||}, Zhongmin Jin^{**}, John D. Lambris[§], and Brian V. Geisbrecht^{†3}

From the [†]School of Biological Sciences, University of Missouri-Kansas City, Kansas City, Missouri 64110, the [§]Department of Pathology and Laboratory Medicine, University of Pennsylvania, Philadelphia, Pennsylvania 19105, the [¶]Department of Medicine, The Johns Hopkins University, Baltimore, Maryland 21224, the ^{||}Center for Bioinformatics and Computational Biology, University of Maryland, College Park, Maryland 20742, and the ^{**}Advanced Photon Source, Argonne National Laboratory, Argonne, Illinois 60439

We report here the discovery and characterization of Ehp, a new secreted *Staphylococcus aureus* protein that potently inhibits the alternative complement activation pathway. Ehp was identified through a genomic scan as an uncharacterized secreted protein from *S. aureus*, and immunoblotting of conditioned *S. aureus* culture medium revealed that the Ehp protein was secreted at the highest levels during log-phase bacterial growth. The mature Ehp polypeptide is composed of 80 residues and is 44% identical to the complement inhibitory domain of *S. aureus* Efb (extracellular fibrinogen-binding protein). We observed preferential binding by Ehp to native and hydrolyzed C3 relative to fully active C3b and found that Ehp formed a subnanomolar affinity complex with these various forms of C3 by binding to its thioester-containing C3d domain. Site-directed mutagenesis demonstrated that Arg⁷⁵ and Asn⁸² are important in forming the Ehp-C3d complex, but loss of these side chains did not completely disrupt Ehp/C3d binding. This suggested the presence of a second C3d-binding site in Ehp, which was mapped to the proximity of Ehp Asn⁶³. Further molecular level details of the Ehp/C3d interaction were revealed by solving the 2.7-Å crystal structure of an Ehp-C3d complex in which the low affinity site had been mutationally inactivated. Ehp potently inhibited C3b deposition onto sensitized surfaces by the alternative complement activation pathway. This inhibition was directly related to Ehp/C3d binding and was more potent than that seen for Efb-C. An altered conformation in Ehp-bound C3 was detected by monoclonal antibody C3-9, which is specific for a neoantigen exposed in activated forms of C3. Our results suggest that increased inhibitory potency of Ehp relative to Efb-C is derived from the second C3-binding site in this new protein.

Staphylococcus aureus is a widely disseminated and persistent human pathogen that has a long-standing and increasingly negative impact on human health. It is the primary cause of numerous disorders that range from the seemingly mild (such as skin and soft-tissue infections) to several potentially fatal conditions (such as bacteremia, necrotizing pneumonia, and endocarditis) as well as infections associated with implanted medical devices (such as intravascular catheters, pacemakers, and delivery pumps) (1). One of the most striking features of *S. aureus* biology is its ability to survive and colonize distinct microenvironments within the host organism, and this propensity clearly contributes to its ability to form long-lasting and repetitive infections (1). To facilitate host colonization, *S. aureus* expresses a diverse array of virulence-determining factors, including exoenzymes, toxins, and numerous protein adhesins. These adhesins (termed receptins (2, 3) or MSCRAMM[®] proteins (3)) are believed to contribute to the initiation and propagation of infections by precluding bacterial clearance by physical forces.

Over the last several years, it has also become clear that *S. aureus* produces a series of immunomodulators that promote virulence by affecting both arms of the host immune system (4, 5). Components of the innate immune system represent the first line of defense against infection, and *S. aureus* has consequently evolved modulators of this system (5). In regard to cell-mediated innate immunity, a secreted chemotaxis inhibitory protein from *S. aureus* (CHIPS) that blocks function of the C5a and formylated peptide receptors required for chemotaxis or neutrophils was recently described (6). In terms of humoral innate immunity, the circulating complement system is a primary target of virulence factors produced by many pathogens, including bacteria, viruses, and fungi (7–9), and because the complement component C3 serves a central role in the amplification of all three complement pathways, it is an attractive target for inhibition or modulation of this essential immune response (5, 10). Indeed, SCIN, a secreted complement inhibitory protein from *S. aureus* that effects the function of C3 convertases, was identified late in 2005 (11), and a C3-binding and complement inhibitory activity was recently described for the secreted *S. aureus* extracellular fibrinogen-binding protein Efb (5, 12). Together, these examples illustrate that inhibiting the normal function of the innate immune system is fundamentally important to the success of *S. aureus* as a human pathogen.

Three lines of current evidence suggest that *S. aureus* may

* This work was supported by the School of Biological Sciences, University of Missouri, Kansas City; Grant 2509 from the University of Missouri Research Board (to B. V. G.); and NIAID Grant AI30040 from the National Institutes of Health (to J. D. L.). The costs of publication of this article were defrayed in part by the payment of page charges. This article must therefore be hereby marked "advertisement" in accordance with 18 U.S.C. Section 1734 solely to indicate this fact.

The atomic coordinates and structure factors (code 2NOJ) have been deposited in the Protein Data Bank, Research Collaboratory for Structural Bioinformatics, Rutgers University, New Brunswick, NJ (<http://www.rcsb.org/>).

[†] These authors contributed equally to this work.

² Present address: Advanced Light Source, Lawrence Berkeley National Laboratory, Berkeley, CA 94720.

³ To whom correspondence should be addressed: Div. of Cell Biology and Biophysics, School of Biological Sciences, University of Missouri-Kansas City, 5100 Rockhill Rd., Kansas City, MO 64110. Tel.: 816-235-2592; Fax: 816-235-1503; E-mail: GeisbrechtB@umkc.edu.

Identification of *S. aureus* Ehp

express additional complement inhibitory proteins, the functions of which are not yet appreciated. First, *S. aureus* has been shown to activate all three complement pathways (13–17), and mice that have been complement-depleted by treatment with cobra venom factor succumb quickly to staphylococcal bacteremia (18). This underscores the importance of complement inhibition in *S. aureus* virulence. Second, complement proteins are among the most abundant components in human plasma (19, 20). This makes it unlikely that any single complement inhibitory protein could be expressed by the pathogen at levels sufficient to provide a completely effective mode of protection from complement-mediated opsonophagocytosis. Finally, the numerous functions of C3, along with their accompanying regulatory mechanisms, provide many different locations at which inhibitory strategies could be executed (10). Indeed, although SCIN and Efb both block complement activation, their mechanisms of action appear to be completely distinct (11, 21).

To explore the possibility that *S. aureus* may express additional proteins that act on the human immune response, we recently conducted an *in silico* screen to identify uncharacterized secreted proteins of *S. aureus*.⁴ Using this approach, we identified the protein SAV1155, the further characterization of which we report here. SAV1155 was expressed at the highest levels during log-phase culture growth, displayed a high level of sequence identity to Efb, and formed a subnanomolar affinity complex with human complement component C3. Functional analysis of SAV1155 demonstrated that it potently inhibited the alternative pathway of complement activation by perturbing the solution conformation of C3. On the basis of these properties, we have tentatively assigned the name Ehp (for Efb homologous protein) to SAV1155. Our results support previous work that identified induced conformational change in C3 as a novel basis for complement inhibition and elaborate upon both the structure and function of a growing family of small secreted complement inhibitory proteins from *S. aureus* (22).

EXPERIMENTAL PROCEDURES

Protein Expression and Purification—A designer gene fragment encoding residues 30–109 of Ehp was amplified from *S. aureus* genomic DNA by PCR using oligonucleotides 5'-aaagtcgacccaactaaaaacgttgaagctgctaaaaatgatgacag-3' and 5'-tttg-cggccgctattttaaagtattatattttaaactagatcgattgtct-3' as sense and antisense primers, respectively. These oligonucleotides appended SalI and NotI restriction endonuclease sites at the 5'- and 3'-ends of the amplified Ehp-encoding sequence, and the amplified DNA was digested and cloned into the corresponding sites of the prokaryotic expression vector pT7HMT (23). Following verification of the Ehp-encoding region, this expression vector was transformed into *Escherichia coli* strain BL21(DE3) for recombinant protein expression. Expression, refolding, and purification of Ehp were carried out according to the general protocol reported previously (23). Ehp purified in this fashion was >95% pure as judged by SDS-PAGE and Coomassie Blue staining, migrated as a monomeric 11,000-Da species as judged by analytical gel filtration chromatography, and had an experimental molecular mass of 9809.09 Da (predicted

molecular mass of 9803.37 Da) according to matrix-assisted laser desorption ionization time-of-flight mass spectrometry. The increased molecular mass of recombinant Ehp over that of the predicted mature form of the protein was due to the presence of three additional residues (-GST-) at its N terminus that resulted from the subcloning procedure.

Site-directed mutagenesis of Ehp was carried out according to the two-step megaprimer PCR method (24). Following expression and purification, the structural integrity of all mutants was confirmed by analytical gel filtration chromatography and comparative circular dichroism spectropolarimetry with wild-type Ehp as described previously (23).

A DNA fragment encoding residues 996–1287 of human C3 was amplified via PCR to encode the C1010A mutation and subcloned into a modified form of pET28a lacking all tags. This vector encodes the additional residues MGRST- at its N terminus, and the C1010A mutation is necessary to avoid the formation of the reactive thioester bond found in native C3 (10, 25). Protein expression and purification of this recombinant C3d were carried out according to the general protocol described by Nagar *et al.* (25), with the exception that microfluidization was used to lyse the induced cells (23). Recombinant C3dg was expressed in *E. coli* based on a method described previously (26); here, the pET30 vector containing an S-tag was used instead of a pET11b vector with a T7 epitope tag, and no biotinylation signal peptide was included. C3, C3(H₂O) (hydrolyzed), C3b, and C3c were all prepared according to established protocols (21, 27). Recombinant Efb, Efb-C, and Efb-C(R131E/N138E) were expressed and purified as described previously (21, 23).

Bacterial Culture and Analysis of Conditioned Medium—*S. aureus* strain Mu50 was purchased from American Type Culture Collection and cultured in LB broth in a 37 °C shaking incubator. To analyze the proteins present in the conditioned culture medium at various time points, a 5-ml preculture was diluted into 50 ml of sterile LB broth to achieve an initial $A_{600\text{ nm}}$ of 0.1. Samples equivalent to 1.0 $A_{600\text{ nm}}$ unit were withdrawn and sterile-filtered at 2, 4, 6, 10, 18, 24, and 48 h post-dilution. Following normalization of the volume for the density of the culture, each sample was concentrated to 0.2 ml in an Amicon centrifugal concentrator (5000 nominal M_r cutoff). 20 μ l of each sample was separated by 4–20% SDS-PAGE and processed for immunoblotting as described (21, 28).

Antibodies and Immunoblotting—Purified recombinant Ehp was used to elicit the production of anti-Ehp polyclonal antibodies in guinea pigs. Guinea pigs were purchased from and maintained and immunized according to the standard protocols of Spring Valley Laboratories, Inc. (Woodbine, MD). For affinity purification, 100 μ l of post-immune serum was diluted 1:10 in phosphate-buffered saline (PBS)⁵ and 0.1% (v/v) Tween 20 (PBST) and applied by gravity flow to a 1-ml column containing 1 mg of Ehp immobilized on CNBr-Sepharose fast flow (GE Healthcare) according to the manufacturer's suggestions.

⁴ B. V. Geisbrecht and M. Pop, unpublished data.

⁵ The abbreviations used are: PBS, phosphate-buffered saline; LC, liquid chromatography; MS/MS, tandem mass spectrometry; SPR, surface plasmon resonance; MES, 4-merpholineethanesulfonic acid; ELISA, enzyme-linked immunosorbent assay.

After washing with 10 ml of PBST, bound antibodies were eluted by applying 2 ml of 0.1 M glycine (pH 2.0), followed by immediate neutralization with 0.2 ml of 1 M Tris base. The affinity-purified antibodies were dialyzed into PBS and used at a final concentration of 1:100 as the primary probe for immunoblotting according to a previously published procedure (28). Horseradish peroxidase-conjugated rabbit anti-guinea pig secondary antibody was purchased from Sigma.

Pull-down Assays and Proteomics—Ehp, Efb, Efb-C, and Efb-C(R131E/N138E) were immobilized on CNBr-Sepharose fast flow according to the manufacturer's suggestions. The coupling density was 2 mg/ml of resin for all proteins except Efb, which was coupled at 3 mg/ml to account for its larger molecular mass relative to the others. Following quenching of excess reactive groups with 0.2 M Tris-HCl (pH 8.0) for 2 h at 25 °C, the affinity resins were washed and stored as 50% slurries in PBST. To test for binding to plasma proteins, aliquots of EDTA-stabilized human plasma were diluted 1:100 in PBST and mixed individually with 20 μ l of each affinity resin in a total volume of 1 ml. Following a 10-min incubation at 25 °C, the resins were isolated by centrifugation at 3500 \times g for 2 min, and washed five times with 1 ml of PBST. After the last wash, each resin was resuspended in 20 μ l of 2 \times Laemmli sample buffer, mixed briefly, and heated at 95 °C for 5 min. Following sample preparation, the proteins contained in each sample were separated by 4–20% gradient SDS-PAGE and visualized by Coomassie Blue staining. For protein identification, the bands of interest were excised from the gel and subjected to in-gel proteolysis by trypsin as described by Kinter and Sherman (29). The resulting tryptic fragments were extracted, separated by capillary liquid chromatography (LC), and characterized by tandem mass spectrometry (MS/MS) (29). Proteins were identified by comparing the observed fragmentation ion patterns against a data base of human proteins using the MASCOT software package (29).

Surface Plasmon Resonance (SPR)—All SPR experiments were performed on a Biacore 2000 biosensor at 25 °C using running buffer (10 mM sodium phosphate (pH 7.4), 150 mM NaCl, and 0.005% Tween 20) as described previously (21). To examine Ehp binding to C3 and its various fragments, 200–600 response units of Ehp were immobilized on a CM5 sensor chip at a flow rate of 10 μ l/min using amine coupling (5-min activation and deactivation). All C3 fragments were screened at a concentration of 200 nM and at a flow rate of 20 μ l/min with injection and dissociation phases of 3 min each. The Ehp surface was regenerated with two 30-s injections of 0.1% SDS and reconstituted in running buffer for 10 min. An empty flow cell, which was only activated and deactivated, was used as a reference surface. Three buffer blanks were included in each analysis, and their average signals were subtracted from the processed sample responses (double referencing) (30). Data processing and analysis were performed using Scrubber (Version 2.0a, BioLogic Software Pty. Ltd.). The SPR experiments were repeated three times using different immobilization densities and protein batches, essentially leading to the same ranking result. Native C3 was freshly reconstituted from MES-precipitated samples and kept on ice until immediately prior to analysis on the same day. Under these conditions, contamination with C3(H₂O) was found to be <2% (21).

Isothermal Titration Calorimetry—Isothermal titration calorimetry experiments were performed at 25 °C using a VP-ITC calorimeter (MicroCal) as described previously (21). Briefly, all proteins were dissolved in 20 mM Tris (pH 8.0) and 200 mM NaCl to a final concentration of either 150 μ M for *S. aureus* proteins or 12 μ M for recombinant C3d or C3dg. A preliminary 1- μ l injection of the *S. aureus* protein into a solution of C3d was followed by multiple injections of 5 μ l at 240-s intervals, and the evolved heat was measured. After correcting the observed heat values for the effects of dilution and background buffer titration, all processed data were fit using Origin 7.0 software (OriginLab) to either a single- or two-site binding model to give the final experimental values for enthalpy (ΔH), entropy (ΔS), and the equilibrium dissociation constant (K_d).

Complement Inhibition Assays—The abilities of Ehp and its various mutants to inhibit the classical and alternative pathways of complement activation were evaluated using previously described enzyme-linked immunosorbent assay (ELISA) methods (31, 32). For both assays, detection of C3b bound to the wells was achieved using a 1:1000 dilution of horseradish peroxidase-conjugated anti-human C3 antibody (MP Biomedicals). Following extensive washing with PBS containing 0.005% Tween 20, color was developed by addition of the peroxidase substrate 2,2'-azinobis(3-ethylbenzthiazoline-6-sulfonic acid), and absorbance was measured at 405 nm. Percent inhibition was plotted against the protein concentration, and the resulting data set was fit to a logistic dose-response function using Origin 7.0 software. IC₅₀ values were obtained from the fit parameters that achieved the lowest χ^2 value.

C3 Capture ELISA—EDTA-stabilized plasma diluted 1:10 in PBS was incubated with or without 25 μ M Ehp, the various site-directed mutants of Ehp, or controls at 37 °C for 1 h and centrifuged at 3000 rpm for 5 min. The supernatant was added to an ELISA plate coated with monoclonal antibody C3-9 (2 μ g/ml), which recognizes a neoantigen that is exposed in C3(H₂O), C3b, and C3c, but not in native C3 (33, 34). The wells were washed twice with PBS containing 0.005% Tween 20 and incubated with rabbit anti-C3a polyclonal antibody (2 μ g/ml) that had been affinity-purified on a CNBr-Sepharose column derivatized with an N-terminal C3a peptide (H-SVQLTEKRM-DKVGKYPKELRK-NH₂) (33, 34). Detection of bound anti-C3a antibody was performed using horseradish peroxidase-conjugated goat anti-rabbit IgG antibody (1:1000) and the peroxidase substrate 2,2'-azinobis(3-ethylbenzthiazoline-6-sulfonic acid) by measuring the absorbance at 405 nm. Values were plotted against the protein concentration, and the resulting data set was fit to a logistic dose-response function using Origin 7.0 software.

Crystallization, Data Collection, Structure Solution, Refinement, and Analysis—The Ehp(N63E)·C3d complex was reconstituted from purified monomers and isolated by gel filtration chromatography on a Superdex 75 (26/60) column (GE Healthcare). Following purification, the complex was dialyzed against double-distilled H₂O and concentrated to 13 mg/ml complex by centrifugal ultrafiltration. Twinned needle cluster crystals of the complex were obtained by vapor diffusion of hanging drops consisting of equal volumes of 13 mg/ml Ehp(N63E)·C3d and a mother liquid of 0.2 M Li₂SO₄, 25% polyethylene glycol 3350,

Identification of *S. aureus* Ehp

and 0.1 M Tris-HCl (pH 8.2). Although the original crystals did not diffract x-rays, inclusion of 0.2 M CaCl₂ as an additive in the mother liquid occasionally resulted in clusters with blades of sufficient thickness to allow their manipulation and a more thorough diffraction analysis. The Ehp(N63E)·C3d crystals appeared within 7 days and belonged to the space group $P2_1$, with cell dimensions of $a = 67.89$, $b = 91.03$, and $c = 122.60$ Å and $\beta = 89.93^\circ$ and four complete complexes in the asymmetric unit, which corresponded to a solvent content of 44.5%. The structure of Ehp(N63E)·C3d was solved by molecular replacement using x-ray diffraction data to 2.7-Å limiting resolution collected from a single frozen crystal at Southeast Regional Collaborative Access Team beamline 22-ID of the Advanced Photon Source of Argonne National Laboratory. Following data processing using the HKL2000 software package, molecular replacement was carried out with the refined structure of Efb·C·C3d as a search model (Protein Data Bank Code 2GOX) (21) using the program MOLREP (35). Initial phase improvement was carried out using solvent flattening by the program DM (35), and stepwise model building, water addition, and refinement were carried out using the programs O (36) and CNS (37). The final model was attained following TLS refinement in REFMAC5 (38, 39) and consists of residues 975–1265 of human C3 (chain A in the Protein Data Bank file), residues 52–109 of Ehp (chain B in the Protein Data Bank file), and 71 ordered water molecules. No interpretable density was visible for the vector-encoded residues MGSRST in C3d or for residues 30–51 in any Ehp molecules in the refined structure. Additional details on weak density and residues/atoms that could not be modeled can be found in the Protein Data Bank file. Intramolecular distances for protein chains were calculated using the CCP4 suite (35). Structural superpositions of proteins were carried out by the local global alignment method using default parameters (as2ts.llnl.gov/) (40). Representations of protein structures were prepared using PyMOL (pymol.sourceforge.net). The refined coordinates and structure factors (code 2NOJ) for the Ehp(N63E)·C3d complex have been deposited in the Protein Data Bank.

Miscellaneous—The numbering schemes for Ehp (GenBank™ accession number NP_371679), Efb (accession number P68799), and human C3 (accession number P01024) presented here reflect sequence positions in the respective preproteins. Multiple sequence alignments of proteins were produced by ClustalW and rendered using ESPrpt (esprpt.ibcp.fr). Purified human fibrinogen was obtained from Sigma (catalog no. F-3879). The compstatin analog used in this study was 4(1MeW)7W and has been described previously by Katragadda *et al.* (41).

RESULTS

Identification of SAV1155/Ehp as an Uncharacterized C3-binding Protein from *S. aureus*—The orphan protein SAV1155 was identified during a genome-wide screen for all proteins in *S. aureus* that were predicted to contain a type 1 signal peptide at their N terminus.⁴ The SAV1155 open reading frame encodes a 109-residue polypeptide with a high probability signal peptidase site between residues 29 and 30 (www.cbs.dtu.dk/services/SignalP/) and was predicted to yield

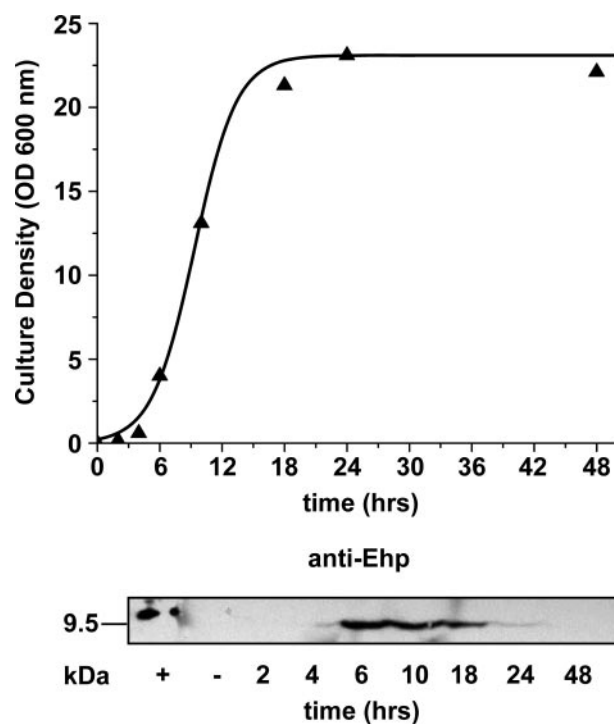


FIGURE 1. Ehp (SAV1155) is secreted at the highest levels during log-phase growth. *S. aureus* cells were grown in liquid culture at 37 °C, and samples of the conditioned medium were withdrawn at the various time points shown (upper panel). After normalizing each sample for culture density, the conditioned medium was concentrated by ultrafiltration, separated by SDS-PAGE, and processed for immunoblotting with affinity-purified anti-Ehp antibodies (lower panel). The molecular mass of Ehp is indicated, along with polyhistidine-tagged Ehp (positive control; +) and sterile culture medium (negative control; -). The higher apparent mass of the positive control (+) is due to the presence of the fusion tag that is not found on natively expressed Ehp.

an 80-residue mature protein with a deduced molecular mass of 9558 Da. The theoretical isoelectric point of SAV1155 is also notably basic ($pI \sim 10.78$) and reflects the preponderance of lysine residues in the sequence (15/80 positions). To determine whether SAV1155 is in fact secreted from *S. aureus* cells, we raised polyclonal antisera in guinea pigs against a recombinant form of SAV1155 corresponding to the entire predicted mature protein; then, following affinity purification, we used these antibodies to test for the presence of SAV1155 in the growth medium of an *S. aureus* culture at various time points (Fig. 1). We observed that SAV1155 was efficiently secreted in the medium. Although the highest levels of Ehp were present during log-phase growth (6–18 h), secreted Ehp was still detectable at times immediately preceding (4 h) and following (24 h) this period. This result demonstrates that SAV1155 is expressed and secreted from actively growing *S. aureus* cells and suggests that this protein may have an important but yet unappreciated function.

Because no functional data were available on SAV1155, we examined the relationship of this protein to previously characterized molecules on the basis of sequence similarity. BLAST searches of the non-redundant protein data base revealed a surprising homology between SAV1155 and the 16-kDa Efb protein from *S. aureus* (42, 43). Subsequent ClustalW sequence alignment of Ehp and Efb indicated that the region of homology between these proteins is confined to the C-terminal C3 inhib-

Identification of *S. aureus* Ehp

parameters associated with Ehp/C3d binding. As shown in Fig. 4*a* and Table 1, titration of Ehp into a fixed quantity of C3d resulted in a peculiar two-site ligand in the cell binding iso-

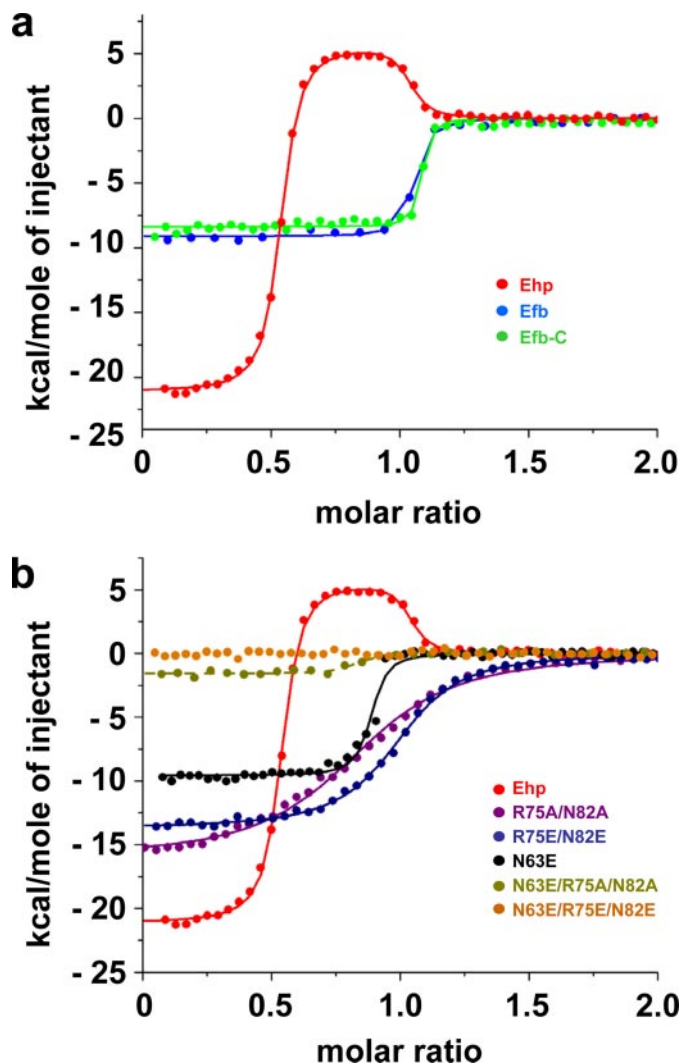


FIGURE 4. Asn^{63} , Arg^{75} , and Asn^{82} of Ehp are important in forming the Ehp-C3d complex. *a*, the thermodynamics of the Ehp/C3d interaction were assessed by isothermal titration calorimetry. The data presented were fit to titration models for titration of Ehp, Efb, and Efb-C into a solution of recombinant C3d. Note the presence of a second phase in the Ehp-C3d titration curve, which was fit to a two-site binding model. *b*, shown are the results from the calorimetric analysis of C3d binding for site-directed mutants in Ehp. The experimental values for thermodynamic constants for each titration are presented in Table 1.

TABLE 1
Characterization of Ehp/C3d binding by isothermal titration calorimetry

Titratant	Cell	<i>n</i>	K_d	ΔH	ΔS
			<i>nM</i>	<i>kcal/mol</i>	<i>cal/mol/K</i>
Ehp ^a	C3d	0.94 ± 0.01	0.18	-8.75 ± 0.06	15.3
Ehp ^b	C3d	0.86 ± 0.01	125	-14.73 ± 0.12	-17.8
C3dg ^a	Ehp	1.06 ± 0.00	0.08	-7.13 ± 0.05	22.4
C3dg ^b	Ehp	0.98 ± 0.01	80	-13.61 ± 0.08	-13.2
R75A/N82A	C3d	0.86 ± 0.00	730	-16.02 ± 0.15	-25.6
R75E/N82E	C3d	0.99 ± 0.00	240	-13.71 ± 0.07	-15.7
N63E	C3d	0.87 ± 0.00	13	-9.46 ± 0.09	4.3
N63E/R75A/N82A	C3d	0.69 ± 0.02	46	-2.14 ± 0.09	26.4
N63E/R75E/N82E	C3d	ND ^c		ND	

^a Titration fit to a two-site model; values shown for the first site.

^b Titration fit to a two-site model; values are shown for the second site.

^c ND, binding not detectable using this assay.

therm that exhibited transition points at Ehp/C3d molar ratios of ~0.5 and 1.0. The first site was exothermic ($\Delta H = -8.75$ kcal mol⁻¹) and fit to an equilibrium dissociation constant (K_d) of 0.18 nM (Table 1). Although the second isotherm was also substantially exothermic ($\Delta H = -14.7$ kcal mol⁻¹), this site fit to a lower affinity K_d value of 125 nM as a result of a significant entropic penalty relative to the first site. We ruled out the likelihood that this observation might have arisen from an experimental artifact by performing an analogous study in which C3dg was titrated into a solution of Ehp. Again, we observed an entropically favored higher affinity site, along with an entropically opposed weaker site (Table 1). Furthermore, the observation that the Ehp/C3d interaction saturated at a 1:1 molar ratio when C3d was limiting but at a 2:1 molar ratio when Ehp was limiting strongly suggests that both C3d-binding sites in Ehp recognize the same region within C3d.

The crystal structure of Efb-C bound to C3d identified Arg¹³¹ and Asn¹³⁸ as the two residues critical to formation of this complex (21), and because Ehp Arg⁷⁵ and Asn⁸² aligned with these positions in Efb-C, we examined their contributions to formation of the Ehp-C3d complex using site-directed mutagenesis (Fig. 4*b* and Table 1). Mutation of both Arg⁷⁵ and Asn⁸² to alanine or glutamate resulted in single-site binding curves with enthalpic and entropic terms comparable with those of the second, lower affinity binding site in Ehp described above. Although this indicated that loss of these residues abolished one binding site in Ehp that shared many of the characteristics observed previously for Efb-C (21), it was notable that the C3d binding by both Ehp double mutants was still significant even though the corresponding Efb-C double mutants did not bind C3d. This raised questions regarding the nature of the residual affinity of Ehp for C3d and of the molecular basis for the second C3d-binding site in Ehp.

We subsequently examined the Ehp sequence and noticed two tandem repeats of the heptamer peptide -AQ(K/R)AVNL-between residues 58 and 64 and residues 77 and 83 (Fig. 2*a*). Although both repeats contain an asparagine residue that corresponds to Asn¹³⁸ in Efb-C, the first heptapeptide sequence lacks the corresponding arginine residue that is found at the Efb-C-C3d complex interface and that we have shown by mutagenesis to be important to Ehp/C3d binding (Fig. 4*b* and Table 1). Nevertheless, we hypothesized that this additional repeat sequence may still be important in forming the Ehp-C3d complex. To test this directly, we generated an N63E mutant, as

well as the analogous series of Ehp double mutants described above in the N63E background, and monitored the binding isotherms of these proteins to C3d using calorimetry (Fig. 4b and Table 1). Conversely to the previous sets of mutations, change of Asn⁶³ alone to glutamate resulted an entropically favored, single-site binding curve ($\Delta H = -9.46 \text{ kcal mol}^{-1}$) that instead resembled that of Efb-C alone (21). The N63E/R75A/N82A triple mutant evolved only $-2.14 \text{ kcal mol}^{-1}$ of enthalpy upon binding to C3d. This particular mutant also had an unexpectedly low K_d value of 46 nM, which probably resulted from slight inaccuracy in the fit caused by such a comparatively small signal in the calorimetric assay. Finally, when all three positions were mutated to glutamate simultaneously, no binding to C3d was detected. Together, these results suggest that two distinct sites on the Ehp protein are important determinants in C3d recognition.

Ehp Inhibits Complement Activation by Binding to C3d and Inducing Conformational Change in C3—To gain a better understanding of Ehp function, we measured the effects of Ehp/C3 binding on a series of functional assays that measured generation and deposition of C3b through either the classical or alternative pathway (Fig. 5a). We observed potent, dose-dependent inhibition of the alternative complement activation pathway by Ehp ($IC_{50} \sim 120 \text{ nM}$ Ehp). Interestingly, the inhibitory properties of Ehp were ~ 2 – 3 -fold greater than those of Efb or compstatin, a complement inhibitory cyclic 13-mer peptide that has undergone several rounds of combinatorial optimization (21, 45–47). Furthermore, alternative pathway inhibition by Ehp correlated directly with C3d binding because the Ehp mutants described above had reduced inhibitory properties that reflected their individual affinities for C3d (Fig. 5a and Table 1). This indicated that the effect of Ehp on the alternative pathway was a direct result of its ability to bind to C3. On the other hand, inhibition of classical pathway activation was seen only at unphysiologically high concentrations of Ehp (data not shown). Amplification of the alternative pathway has been shown recently to contribute $>80\%$ of the classical pathway-induced activation of downstream complement components (48). Thus, our observation most likely reflects the inhibitory effects of Ehp on alternative pathway self-amplification.

The results from the experiments described above revealed that Ehp blocked the alternative complement activation pathway by forming a subnanomolar affinity complex with C3. To further define the effects of Ehp binding to C3 and its inhibition of the alternative pathway, we incubated C3 in human plasma with Ehp, the site-directed Ehp mutants described in Table 1, or buffer alone and examined the reactivity of each sample over a 1000-fold dilution series in a capture ELISA method against a panel of monoclonal antibodies specific for the particular compositions and conformations of C3 and/or the various intermediates of its activation and degradation pathways (33). Incubation of plasma C3 with Ehp resulted in a marked increase in the reactivity of bound C3 with monoclonal antibody C3-9 (Fig. 5b), which detects a neoantigen that becomes exposed during C3 activation to C3(H₂O) and C3b (49). This effect was not observed for the site-directed Ehp mutants that were impaired in their ability to bind C3, as these samples reacted

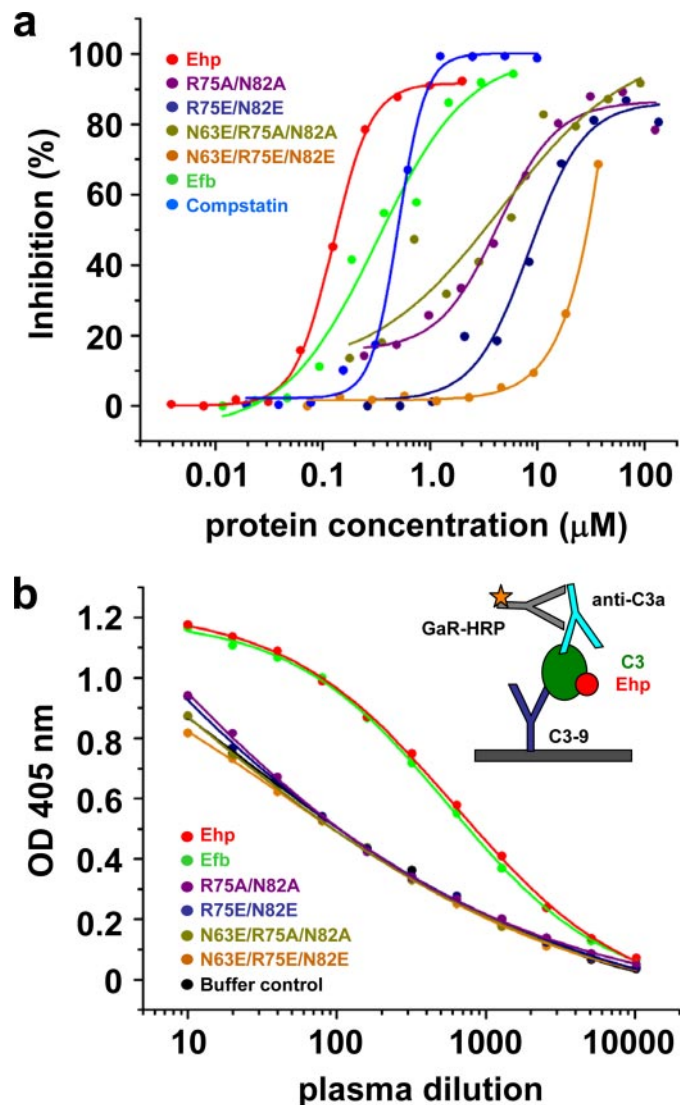


FIGURE 5. Ehp inhibits the alternative pathway of complement activation by altering the solution conformation of C3. *a*, the effect of Ehp and its various site-directed mutants on the alternative pathway of complement activation was examined by ELISA. Experimental data were fit to a dose-response model for each protein. *b*, the Ehp-induced conformational changes in plasma C3 were examined by capture ELISA. Diluted EDTA-stabilized plasma was incubated for 1 h at 37 °C with the proteins described for *a* or with buffer alone, followed by capture on ELISA plates coated with monoclonal antibody C3-9. Bound C3 was detected by incubation with affinity-purified anti-C3a antibodies, followed by horseradish peroxidase-conjugated goat anti-rabbit antibodies (GaR-HRP). The increased reactivity of Ehp-C3 with monoclonal antibody C3-9 is indicative of an active-like conformation in C3, even though the C3a domain has not been proteolytically removed to generate C3b.

with monoclonal antibody C3-9 to essentially the same extent as did C3 treated with buffer alone. Furthermore, the fact that Ehp-bound C3 captured in this manner was recognized by both C3a- and C3b-specific antibodies (Fig. 5b) (data not shown) throughout the entire dilution series indicated that this C3 was not being processed into C3b, but instead suggested that Ehp binding altered the conformation of C3 and increased exposure of the C3-9-specific epitope. Indeed, the reactivity of Ehp-C3 against monoclonal antibody C3-9 was nearly indistinguishable from that of Efb-C3 (Fig. 5b), and there is strong evidence for induction of C3 conformational changes following Efb binding (21).

Identification of *S. aureus* Ehp

The 2.7-Å Crystal Structure of the Ehp-C3d Complex Shares Many Features with that of Efb-C-C3d

—During the course of this study, we obtained co-crystals of the Ehp(N63E)·C3d complex that diffracted to 2.7-Å limiting resolution. We chose to study the N63E mutant of Ehp because this mutation eliminated the second, lower affinity binding site (Table 1) and resulted in a homogenous preparation of protein complexes as judged by gel filtration chromatography (data not shown). The structure of this complex was solved by molecular replacement and refined to 2.7-Å limiting resolution, with R_{cryst} and R_{free} values of 29.0 and 28.4%, respectively (Fig. 6 and Table 2). Our observation that Ehp(N63E) still bound C3d with a K_d value near those of wild-type Ehp and Efb-C (Tables 1 and 2) suggests that this structure reflects many of the important binding properties of Ehp, with the obvious exception being the second, lower affinity binding site of Ehp described above (Fig. 4 and Table 1). Even though Ehp shares a moderate level sequence identity of 44% with Efb-C, this complex displays a large amount of structural identity to Efb-C bound to C3d (21). Comparison of these two individual complexes revealed that 344 of the 355 C- α positions in Ehp(N63E)·C3d superimpose within a 2.5-Å distance onto the 362 residues in Efb-C·C3d with a root mean square deviation of 0.72 Å. Although numerous ancillary interactions between the Ehp and C3d polypeptides were seen, we observed extensive intermolecular contacts between Ehp·C3d that were established by Ehp Arg⁷⁵ and Asn⁸² (Fig. 6b). Here, Arg⁷⁵ appears to serve as the cornerstone for a network of polar interactions composed of three different residues, whereas the side chain amide of Asn⁸² is well positioned to bind the backbone atoms of Val¹⁰⁹⁰, Ile¹⁰⁹³, and Ile¹⁰⁹⁵ of C3d. It is noteworthy that Arg⁷⁹ appears to serve a role in orienting the interactions of Arg⁷⁵. This inter-

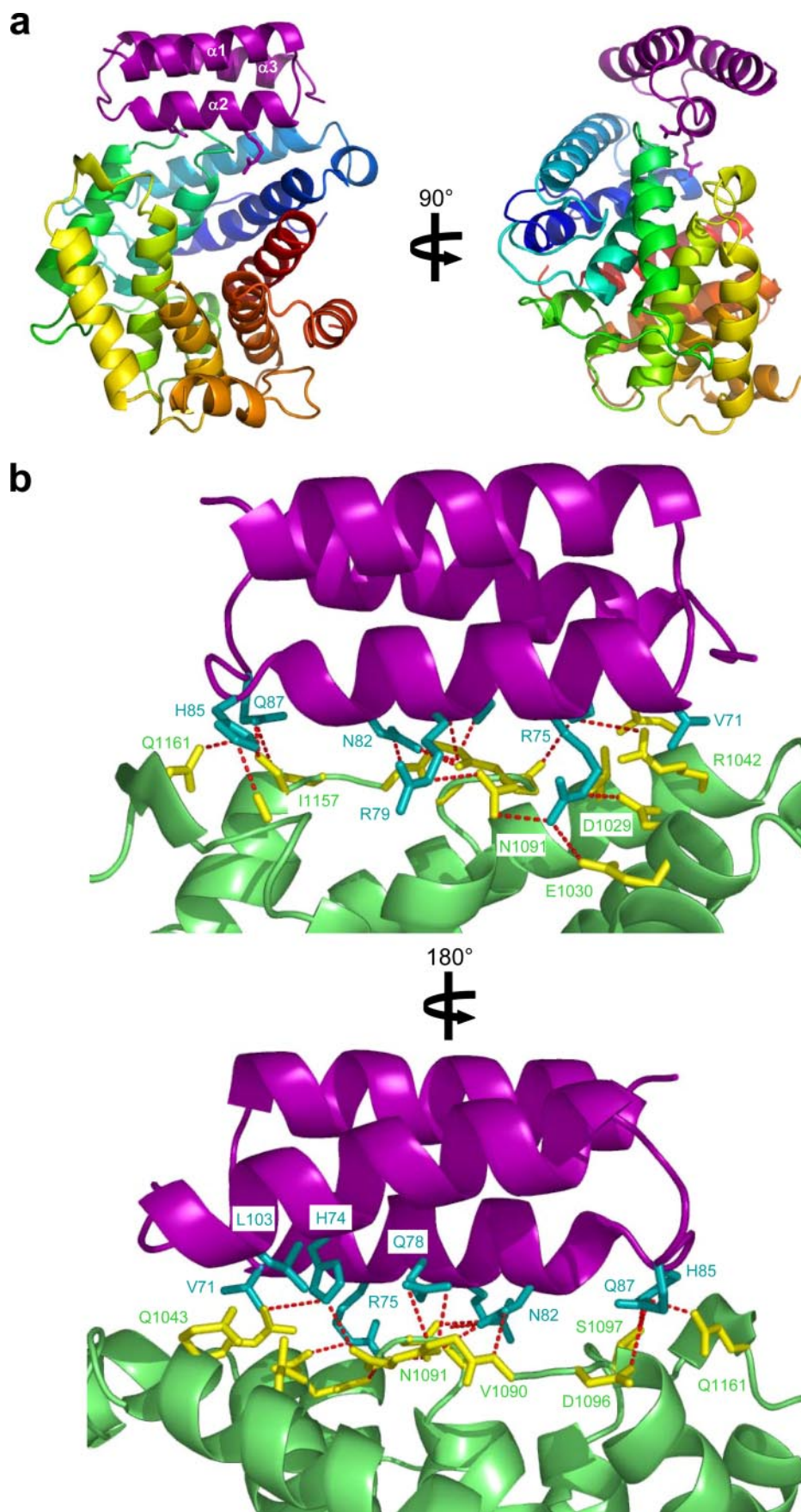


TABLE 2
Diffraction data collection statistics and structural refinement

The refined coordinates and structure factors (code 2NOJ) have been deposited in the Protein Data Bank. APS, Advanced Photon Source; ASU, asymmetric unit; r.m.s.d., root mean square deviation.

Data collection	
Beamline, wavelength (Å)	APS 22-ID, 0.9184
Space group	$P2_1$
Unit cell dimensions	$a = 67.89, b = 91.03, c = 122.60$ Å; $\beta = 89.93^\circ$
Complexes/ASU	4
Resolution limits (Å)	50 to 2.7
Completeness (%)	80.8 (73.3)
Unique reflections	33,242
Multiplicity	2.5
$R_{\text{merge}}(\%)^a$	18.9 (57.2)
$\langle I \rangle / \langle \sigma I \rangle$	3.7 (2.1)
Refinement statistics	
$R_{\text{cryst}}/R_{\text{free}}(\%)^b$	29.0/28.4
r.m.s.d. from ideal	
Bond length (Å)	0.010
Bond angle	1.34°
Average B factor	
All atoms (Å ²)	48.51
Water (Å ²)	25.73
Ramachandran core (disallowed; %)	99.8 (0)
Protein atoms modeled	9705
Ordered solvent molecules	71

^a $R_{\text{merge}} = \sum_i \sum_h |I_i(h) - \langle I(h) \rangle| / \sum_i \sum_h I_i(h)$, where $I_i(h)$ is the i th measurement of reflection h and $\langle I(h) \rangle$ is a weighted mean of all measurements of h .

^b $R = \sum_h |F_o(h) - F_c(h)| / \sum_h F_o(h)$. R_{cryst} and R_{free} were calculated from the working and test reflection sets, respectively. The test set constituted 5% of the total reflections not used in refinement.

action is not observed in the Efb-C-C3d complex because the equivalent position in Efb-C is a lysine and lacks the essential N- ϵ atom. Thus, this structure accounts well for the site-directed mutagenesis data shown in Fig. 4 and Table 1 and also reflects the conserved contributions of the arginine and asparagine residues within the high affinity C3d-binding site shared between Ehp and Efb-C.

DISCUSSION

To further our understanding of the interactions between *S. aureus* and the human immune system, we undertook a genome-based approach to identify secreted proteins of unknown function that may function in immunosuppressive or anti-inflammatory capacities. Using this approach, we identified Ehp and demonstrated that it is a potent inhibitor of the alternative pathway of complement activation. Because activation of the alternative pathway is stimulated by a variety of viruses, fungi, protozoans, and bacteria, it was reasonable to expect that *S. aureus* would have evolved or achieved sophisticated mechanisms to inhibit this essential component of the host immune system. It is interesting that this organism appears to have arrived at a complement inhibitory strategy distinct from most pathogens that relies on secreted molecules acting at long-range instead of membrane-tethered inhibitors (50, 51). Structure-based multiple sequence alignment indicated that each of these secreted complement inhibitory pro-

teins (including SCIN (11), Efb (5, 12, 21), and Ehp) is characterized by an ~ 65 -residue three-helix bundle motif (Fig. 2a). Yet despite this architectural similarity, the mechanisms used by these respective *S. aureus* proteins are distinct. SCIN mediates innate immune evasion by binding and stabilizing the alternative pathway C3 convertase complex C3bBbP in a surface-specific manner, thereby blocking further C3b opsonization of the bacterial cell surface (11); however, SCIN itself is incapable of binding directly to C3, the central component of the alternative pathway. In contrast, Efb blocks C3b opsonization of the bacterial cell (5) by binding to native unactivated C3, altering its solution conformation, and preventing its maturation into C3b (21). Our data presented here reveal that Ehp shares a similar mechanism with Efb in that it binds native C3 (Figs. 2 and 3 and Table 1), alters the solution conformation of bound C3 (Fig. 5), and blocks C3b deposition onto complement-sensitized surfaces (Fig. 5). The fact that both SCIN (52) and Ehp (Fig. 1) are expressed at early time points in the bacterial growth cycle suggests that these complement inhibitors may act in concert to provide a physiologically useful level of innate immune evasion for *S. aureus* cells (52).

In this study, we have provided independent lines of evidence which strongly suggest that Ehp binding blocks complement activation by altering the solution conformation of native C3 to one that is incompetent to participate in the generation of C3b. On one hand, we observed enhanced reactivity of Ehp-bound C3 with monoclonal antibody C3-9 (33, 49). This enhancement was seen over a wide range of concentrations and was not detected for C3 treated with Ehp mutants that have diminished C3d binding ability (Fig. 5); this indicates that Ehp binding is directly responsible for increased exposure of the C3-9 epitope. Nishida *et al.* (49) recently demonstrated that monoclonal antibody C3-9 binds to macroglobulin domains 7 and 8 of the C3 α -chain, and the recent crystal structures of C3 and C3b have shown that these domains comprise a portion of the “keyring-like” core structure of C3 and become exposed during C3 activation to C3b (53, 54). The fact that Ehp-bound C3 was recognized by anti-C3a antibodies (Fig. 5) suggests further that Ehp binding results in an “active-like” C3 conformation, but one that is not a substrate for processing by the C3bBbP convertase. Separately, it has been known for quite some time that the changing conformations of C3 correlate with changes in affinity for its many ligands (55–57). Along these lines, although the primary Ehp recognition site of C3d remains largely unperturbed in the crystal structures of C3, C3b, and C3d (25, 53, 54), the observed differences in Ehp relative binding affinity shown in Fig. 3 are consistent and reproducible. It is also worth noting that we observed a similar series of binding preferences for Efb-C as well as Efb-C-induced conformational change in activated C3b (21). Together, these results suggest that alteration of both C3 and C3b solution conformations by small binding proteins such as Ehp and Efb represents an important mode of

FIGURE 6. Crystal structure of the Ehp(N63E)-C3d complex at 2.7-Å resolution. *a*, two orthogonal views of the refined Ehp(N63E)-C3d crystal structure are shown as ribbon diagrams. The Ehp chain is shown in purple, whereas C3d is shown in an indexed color scheme, where the N terminus is blue and the C terminus is red. *b*, two opposing views of the intermolecular contacts present in the Ehp(N63E)-C3d complex. Ehp is shown in purple and C3d in green, whereas highlighted side chains donated by Ehp and C3d are presented as blue and yellow stick models, respectively. Likely polar contacts are represented by dashed red lines.

Identification of *S. aureus* Ehp

innate immune evasion that has been manifested in the form of multiple unique proteins expressed and secreted by a pathogenic organism.

The results we have presented here suggest that a great deal of insight into bacterial complement evasion may be gained by not only understanding the similarities of Ehp and Efb, but by also by appreciating their differences. For example, although Ehp and Efb share a common inhibitory mechanism, there seem to be several important distinctions between these two proteins. First, we observed a substantially different binding isotherm for formation of Ehp-C3d compared with either Efb-C3d or Efb-C-C3d by isothermal titration calorimetry. In particular, Ehp displayed an unusual two-site binding curve (Fig. 4 and Table 1). This association of Ehp and C3d is driven by two distinct sites that have distinct thermodynamic properties and that lie on opposing helical faces of the Ehp protein. Our results presented here strongly suggest that although Ehp and Efb-C share a common binding site, the second site unique to Ehp imparts bivalency to this protein when C3d is in molar excess. Second, we found that Ehp was a more potent inhibitor of the alternative pathway than Efb (Fig. 5a). The IC_{50} of Ehp for alternative pathway activation was determined to be ~3-fold lower than the corresponding value reported for Efb(-C) (21). Moreover, the observed IC_{50} values for Ehp and its mutants correlated directly with their affinities for C3d (Fig. 5a and Table 2). The fact that both Efb and Ehp exert their effects by altering the conformation of C3 in a similar manner (this work and Ref. 21) but that Ehp can bind two molecules of C3 suggests that the increased potency of Ehp is likely derived from the ability of this protein to block the function of twice the native C3 molecules as Efb. In this respect, the concentration of native C3 in human plasma (1.2 mg/ml or 6.5 μ M) (10) suggests that the bivalent Ehp-(C3)₂ complex is likely to be the most prevalent complex physiologically.

The crystal structure of the Ehp(N63E)-C3d complex presented in Fig. 6 demonstrates a high degree of identity to that of Efb-C-C3d (21), and both structures indicate that the residues responsible for binding to C3d are concentrated in helix α 2 of Efb-C and Ehp. In particular, the importance of two critical residues in each protein (Arg⁷⁵ and Asn⁸² in Ehp and Arg¹³¹ and Asn¹³⁸ in Efb) has now been established (21). In addition, we have characterized a second C3d-binding site in Ehp that includes Asn⁶³ on helix α 1 and that has now provided further detail on the molecular basis of C3 recognition by these small secreted proteins. The fact that all of these residues are located in such close proximity to one another in both the primary and tertiary structures raises the exciting possibility of developing or screening for molecular mimics of Ehp and/or Efb-C as anti-complement therapeutic candidates. Although it is difficult to predict what sort of molecules would best mimic the interface of these protein/protein interactions *a priori*, the discrete nature of the Ehp-C3d and Efb-C-C3d complex interfaces suggests that such molecules need not be limited to proteins or peptides and may in fact be accessible to the realm of small organic molecules as well. Alternatively, the small size of these proteins, along with the ability to isolate large quantities of them from recombinant strains of *E. coli*, suggests that it may not be unrealistic to develop them into protein-based therapeutic

tics. Although there are obvious challenges to this approach, we have found that the complement inhibitory domains of both Efb-C and Ehp are stable even in the presence of broad-specificity proteases (e.g. subtilisin) (data not shown). These results suggest that proteolytic susceptibility to these molecules is not likely to be an impediment to their use as therapeutic lead substances.

Acknowledgments—We are grateful to the Southeast Regional Collaborative Access Team staff from Advanced Photon Source Sector 22 for technical expertise and assistance during the x-ray diffraction experiments presented here and to the United States Department of Energy for continued access to the Advanced Photon Source. We also thank J. A. Keightley (School of Biological Sciences, University of Missouri, Kansas City) for providing LC-MS/MS identification of C3 and fibrinogen in Fig. 2b and A. Rux and B. Sachais (Department of Pathology, University of Pennsylvania) for support in using the Biacore 2000 instrument. Finally, we thank Steve van Doren and Samuel Bouyain for helpful comments during the preparation of this manuscript.

REFERENCES

1. Lowy, F. D. (1998) *N. Engl. J. Med.* **339**, 520–532
2. Kronvall, G., and Jonsson, K. (1999) *J. Mol. Recognit.* **12**, 1–7
3. Patti, J. M., Allen, B. L., McGavin, M. J., and Höök, M. (1994) *Annu. Rev. Microbiol.* **48**, 585–617
4. Lee, L. Y. L., Miyamoto, Y. J., McIntyre, B. W., Höök, M., McCrean, K. W., McDevitt, D., and Brown, E. L. (2002) *J. Clin. Investig.* **110**, 1461–1471
5. Lee, L. Y. L., Höök, M., Haviland, D., Wetsel, R. A., Yonter, E. O., Syribeys, P., Vernachio, J., and Brown, E. L. (2004) *J. Infect. Dis.* **190**, 571–579
6. de Haas, C. J. C., Veldkamp, K. E., Peschel, A., Weerkamp, F., van Wamel, W. J. B., Heezius, E. C. J. M., Poppelier, M. J. J. G., van Kessel, K. P. M., and van Strijp, J. A. G. (2004) *J. Exp. Med.* **199**, 687–695
7. Wurznner, R. (1999) *Mol. Immunol.* **36**, 249–260
8. Lachmann, P. J. (2002) *Proc. Natl. Acad. Sci. U. S. A.* **99**, 8461–8462
9. Hornef, M. W., Wick, M. J., Rhen, M., and Normark, S. (2002) *Nat. Immunol.* **3**, 1033–1040
10. Sahu, A., and Lambris, J. D. (2001) *Immunol. Rev.* **180**, 35–48
11. Rooijackers, S. H. M., Ruyken, M., Roos, A., Daha, M. R., Prezanis, J. S., Sim, R. B., van Wamel, W. J. B., van Kessel, K. P. M., and van Strijp, J. A. G. (2005) *Nat. Immunol.* **6**, 920–927
12. Lee, L. Y. L., Liang, X., Höök, M., and Brown, E. L. (2004) *J. Biol. Chem.* **279**, 50710–50716
13. Neth, O., Jack, D. L., Johnson, M., Klein, N. J., and Turner, M. W. (2002) *J. Immunol.* **169**, 4430–4436
14. Kawasaki, A., Takada, H., Kotani, S., Inai, S., Nagaki, K., Matsumoto, M., Yokogawa, K., Kawata, S., Kusumoto, S., and Shiba, T. (1987) *Microbiol. Immunol.* **31**, 551–569
15. Bredius, R. G., Driedijk, P. C., Schouten, M. F., Weening, R. S., and Out, T. A. (1992) *Infect. Immun.* **60**, 4838–4847
16. Verbrugh, H. A., Van Dijk, W. C., Peters, R., van der Tol, M. E., and Verhoef, J. (1979) *Immunology* **37**, 615–621
17. Wilkinson, B. J., Kim, Y., Peterson, P. K., Quie, P. G., and Michael, A. F. (1978) *Infect. Immun.* **20**, 388–392
18. Sakiniene, E., Bremell, T., and Tarkowski, A. (1999) *Clin. Exp. Immunol.* **115**, 95–102
19. Schuhard, M., Melm, C., Crawford, A., Chapman, H., Cockrill, S., Ray, K., Mehig, R., Chen, D., and Scott, G. (2005) *Proteomic Technologies Reagents Resource Workshop, Specific Depletion of Twenty High Abundance Proteins from Human Plasma, Chicago, IL, December 12–13, 2005*, NCI, National Institutes of Health, Bethesda, MD
20. Adkins, J. N., Varnum, S. M., Aubery, K. J., Moore, R. J., Angell, N. H., Smith, R. D., Springer, D. L., and Pounds, J. G. (2002) *Mol. Cell. Proteomics* **1**, 947–955
21. Hammel, M., Sfyroera, G., Ricklin, D., Magotti, P., Lambris, J. D., and

- Geisbrecht, B. V. (2007) *Nat. Immunol.* **8**, 430–437
22. Rooijackers, S. H. M., van Kessel, K. P. M., and van Strijp, J. A. G. (2005) *Trends Microbiol.* **13**, 596–601
23. Geisbrecht, B. V., Bouyain, S., and Pop, M. (2006) *Protein Expression Purif.* **46**, 23–32
24. Sakar, G., and Sommer, S. S. (1990) *BioTechniques* **8**, 404–407
25. Nagar, B., Jones, R. G., Diefenbach, R. J., Isenman, D. E., and Rini, J. M. (1998) *Science* **280**, 1277–1281
26. Guthridge, J. M., Rakstang, J. K., Young, K. A., Hinshelwood, J., Aslam, M., Robertson, A., Gipson, M. G., Sarrias, M.-R., Moore, W. T., Meagher, M., Karp, D., Lambris, J. D., Perkins, S. J., and Holers, V. M. (2001) *Biochemistry* **40**, 5931–5941
27. Sahu, A., Soulika, A., Morikis, D., Spruce, L., Moore, W. T., and Lambris, J. D. (2000) *J. Immunol.* **165**, 2491–2499
28. Geisbrecht, B. V., Dowd, K. A., Barfield, R. W., Longo, P. A., and Leahy, D. J. (2003) *J. Biol. Chem.* **278**, 32561–32568
29. Kinter, M., and Sherman, N. E. (2000) *Protein Sequencing and Identification Using Tandem Mass Spectrometry*, Wiley-Interscience, Inc., New York
30. Myszka, D. G. (1999) *J. Mol. Recognit.* **12**, 279–284
31. Kraus, D., Medof, D. E., and Mold, C. (1998) *Infect. Immun.* **66**, 399–405
32. Sfyroera, G., Katragadda, M., Morikis, D., Isaacs, S. N., and Lambris, J. D. (2005) *J. Immunol.* **174**, 2143–2151
33. Hack, C. E., Paardekooper, J., Smeenk, R. J. T., Abbink, J., Eerenber, A. J. M., and Nuijens, J. H. (1988) *J. Immunol.* **141**, 1602–1609
34. Becherer, J. D., Alsenz, J., Esparza, I., Hack, C. E., and Lambris, J. D. (1992) *Biochemistry* **31**, 1787–1794
35. Collaborative Computational Crystallography Project 4 (1994) *Acta Crystallogr. Sect. D* **50**, 760–763
36. Jones, T. A., Zou, J.-Y., Cowan, S. W., and Kjeldgaard, M. (1991) *Acta Crystallogr. Sect. D* **47**, 110–119
37. Brunger, A. T., Adams, P. D., Clore, G. M., DeLano, W. L., Gros, P., Grosse-Kunstleve, R. W., Jiang, J.-S., Kuszewski, J., Nilges, M., Pannu, N. S., Read, R. J., Rice, L. M., Simonson, T., and Warren, G. L. (1998) *Acta Crystallogr. Sect. D* **54**, 905–921
38. Winn, M., Isupov, M., and Murshudov, G. N. (2001) *Acta Crystallogr. Sect. D* **57**, 122–133
39. Murshudov, G. N., Lebedev, A., Vagin, A. A., Wilson, K. S., and Dodson, E. J. (1999) *Acta Crystallogr. Sect. D* **55**, 247–255
40. Zemla, A. (2003) *Nucleic Acids Res.* **31**, 3370–3374
41. Katragadda, M., Magotti, P., Sfyroera, G., and Lambris, J. D. (2006) *J. Med. Chem.* **49**, 4616–4622
42. Boden, M. K., and Flock, J.-I. (1992) *Microb. Pathog.* **12**, 289–298
43. Boden, M. K., and Flock, J.-I. (1994) *Mol. Microbiol.* **12**, 599–606
44. Hammel, M., Ramyar, K. X., Spencer, C. T., and Geisbrecht, B. V. (2006) *Acta Crystallogr. F Struct. Biol. Crystalliz. Comm.* **62**, 285–288
45. Morikis, D., Soulika, A. M., Mallik, B., Klepeis, J. L., Floudas, C. A., and Lambris, J. D. (2004) *Biochem. Soc. Trans.* **32**, 28–32
46. Morikis, D., and Lambris, J. D. (2005) *Structure, Dynamics, Activity, and Function of Compstatin and Design of More Potent Analogs*, Taylor & Francis Group, Boca Raton, FL
47. Mallik, B., Katragadda, M., Spruce, L. A., Carafides, C., Tsokos, C. G., Morikis, D., and Lambris, J. D. (2005) *J. Med. Chem.* **48**, 274–286
48. Harboe, M., Ulvund, G., Vien, L., Fung, M., and Mollnes, T. E. (2004) *Clin. Exp. Immunol.* **138**, 439–446
49. Nishida, N., Walz, T., and Springer, T. A. (2006) *Proc. Natl. Acad. Sci. U. S. A.* **103**, 19737–19742
50. Lindahl, G., Sjobring, U., and Johnsson, E. (2000) *Curr. Opin. Immunol.* **12**, 44–51
51. Zipfel, P. F., Skerka, C., Hellwege, J., Jokiranta, S. T., Meri, S., Brade, V., Kraiczky, P., Noris, M., and Remuzzi, G. (2002) *Biochem. Soc. Trans.* **30**, 971–978
52. Rooijackers, S. H. M., Ruyken, M., van Roon, J., van Kessel, K. P. M., van Strijp, J. A. G., and van Wamel, W. J. B. (2006) *Cell. Microbiol.* **8**, 1282–1293
53. Janssen, B. J. C., Huizinga, E. G., Raaijmakers, H. C. A., Roos, A., Daha, M. R., Ekdahl-Nilsson, K., Nilsson, B., and Gros, P. (2005) *Nature* **437**, 505–511
54. Janssen, B. J. C., Christodoulidou, A., McCarthy, A., Lambris, J. D., and Gros, P. (2006) *Nature* **444**, 213–216
55. Isenman, D. E., and Cooper, N. R. (1981) *Mol. Immunol.* **18**, 331–339
56. Isenman, D. E., Kells, D. I. C., Cooper, N. R., Muller-Eberhard, H. J., and Pangburn, M. K. (1981) *Biochemistry* **20**, 4458–4467
57. Isenman, D. E. (1983) *J. Biol. Chem.* **258**, 4238–4244